

## An Analysis of the $\text{CF}_2$ Emission Spectrum in a $\text{CF}_2\text{Cl}_2$ Plus Metastable He System

Takahiko ISHIGURO,\*\* Yoshiaki HAMADA, and Masamichi TSUBOI\*

Faculty of Pharmaceutical Sciences, The University of Tokyo, Hongo, Bunkyo-ku, Tokyo 113

(Received May 23, 1980)

Ultraviolet chemiluminescence caused by a reaction of metastable He and  $\text{CF}_2\text{Cl}_2$  was observed. Laser-excited single-vibronic-level fluorescence of the  $\text{CF}_2$  radical thus produced was also examined. The main feature in the 250–400 nm region was explained as the  $\text{CF}_2 \tilde{A}^1\text{B}_1-\tilde{X}^1\text{A}_1$  transition. The observed vibrational-level population of  $\text{CF}_2 (\tilde{A}^1\text{B}_1)$  resulting from this reaction exhibits a maximum near  $v'_2=5$ . This fact implies that the product has a FCF angle of about  $104^\circ$ , which is nearly equal to the FCF angle ( $105.4^\circ$ ) of the reactant ( $\text{CF}_2\text{Cl}_2$ ) molecule, rather than to the equilibrium FCF angle ( $122^\circ$ ) of the  $\text{CF}_2 (\tilde{A}^1\text{B}_1)$  itself.

The difluorocarbene radical,  $\text{CF}_2$ , an important transient intermediate in fluorocarbon reactions, has been examined by a great number of researchers.<sup>2)</sup> In 1950 Venkateswarlu first observed an emission spectrum between 239.9 and 342.9 nm which was attributed to the  $\text{CF}_2$  radical.<sup>3)</sup> Its absorption spectrum in the 260 nm region was measured with high dispersion by Mathews in 1967.<sup>4)</sup> According to his rotational analysis, the upper and lower electronic states corresponding to this band system are  $^1\text{B}_1$  and  $^1\text{A}_1$  respectively, and the molecule is bent with  $r_0(\text{CF})=1.32 \text{ \AA}$  and  $\angle\text{FCF}=122.3^\circ$  in the ( $^1\text{B}_1$ ) excited state and with  $r_0(\text{CF})=1.300 \text{ \AA}$  and  $\angle\text{FCF}=104.94^\circ$  in the ground state. The absorption and emission spectra gave vibrational frequencies  $\nu'_2=496 \text{ cm}^{-1}$  and  $\nu'_2=668 \text{ cm}^{-1}$ .

Since then, a debate arose as to the location of the  $\text{CF}_2$  triplet state,  $\tilde{a}^3\text{B}_1$ . Recently, Quach-Tat-Trung *et al.*<sup>5)</sup> noted that an emission band system, 340–450 nm, found in the microwave discharge of  $\text{CF}_2\text{X}_2$  (X=Cl, Br), probably belonged to the  $\text{CF}_2 \tilde{a}^3\text{B}_1-\tilde{X}^1\text{A}_1$  transition. Shortly thereafter, however, Koda<sup>6)</sup> observed a structured emission spectrum in the region 470–720 nm resulting from the reaction with  $\text{O}(^3\text{P})$  and  $\text{CF}_2=\text{CF}_2$ , and tentatively assigned this emission to the  $\text{CF}_2 \tilde{a}^3\text{B}_1-\tilde{X}^1\text{A}_1$  phosphorescence transition. Unfortunately, their discussions are based upon a lower dispersion spectra, and the subject does not yet seem to be fully fixed.

We have observed, with a higher dispersion, an ultraviolet emission spectrum resulting from a reaction of a metastable helium atom and dichlorodifluoromethane  $\text{CF}_2\text{Cl}_2$  ("freon 12") in a discharge flow system. A laser excited single-vibronic-level fluorescence of the  $\text{CF}_2$  radical thus produced was also examined. From the results, a number of new pieces of information have been obtained on the reaction as well as on the  $\text{CF}_2$  molecule itself. These will be reported below.

Our special attention has been focused on the FCF angle of the  $\text{CF}_2(\tilde{A}^1\text{B}_1)$  molecule in the initial stage of the reaction, because its equilibrium FCF angle ( $122.3^\circ$ ) is dramatically different from the FCF angle ( $105.4^\circ$ ) of the reactant  $\text{CF}_2\text{Cl}_2$  molecule.<sup>21)</sup> A discussion on this point will be given, in the present paper, in more detail than those on other points.

## Experimental

The arrangement of the experimental apparatus is shown in Fig. 1. Active species of helium were produced by microwave discharge with a magnetron (2450 MHz, 500 W). The discharge portion was made of a 15 mm i.d. (inside diameter) quartz tube, and the product was admitted into a reaction chamber made of a 40 mm i. d. pyrex tube. The reactant gas, that is  $\text{CF}_2\text{Cl}_2$ , was injected into the reaction chamber through a 0.5 mm i. d. pyrex tube at 15 cm downstream from the discharge portion. The reaction chamber was evacuated with a 500-liter/min mechanical pump.

The pressure in the reaction chamber was measured with a Pirani gauge. The pressure of  $\text{CF}_2\text{Cl}_2$  was about 0.4 Torr (1 Torr=133 Pa), and the total pressure in the reaction chamber was about 1.0 torr. The helium gas was purified by

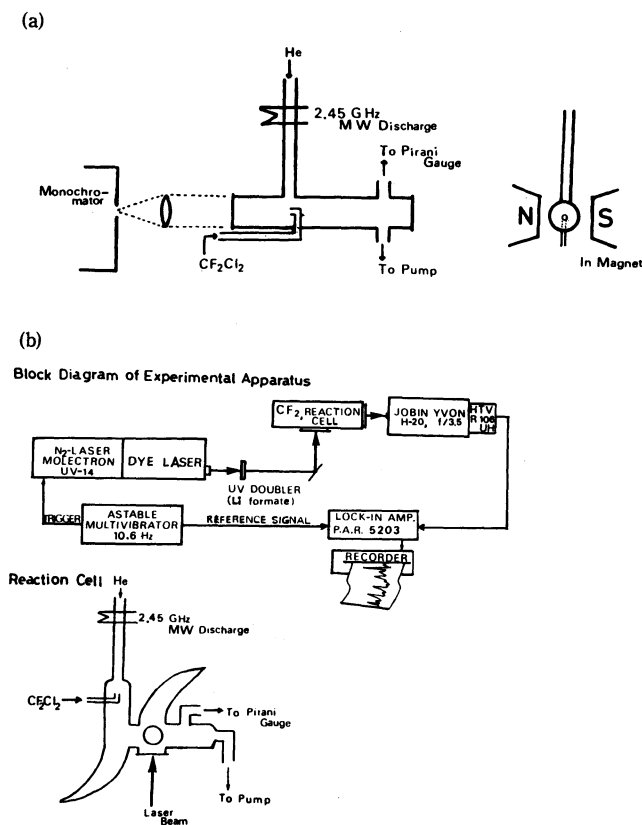


Fig. 1. Experimental set-up (a) for the observation of the  $\text{CF}_2\text{Cl}_2+\text{He}^*$  chemiluminescence and (b) for the single-vibronic-level fluorescence measurement of  $\text{CF}_2$ .

\*\* Present address: Todd Wehr Chemistry Building, Marquette University, Milwaukee, Wisconsin 53233, U.S.A.

passing it through a trap at 77 K before it was introduced into the discharge portion. The  $\text{CF}_2\text{Cl}_2$  gas was purified by the trap to trap distillation method before use.

Emission spectra were observed through a quartz window by a 3.4 m (f) Jarrell-Ash spectrograph. The emission were photographically recorded with exposure times ranging from 8h to 15h on Kodak SA-1 film. The measurements of the spectra were also made by means of a photomultiplier (HTV R106 UH) with the aid of a lock-in amplifier (Princeton Applied Research Model-5203). In case of using the 1st-order diffraction of a 590 grooves/mm (300 nm blaze) grating, the reciprocal dispersion was 0.52 nm/mm. The higher dispersion spectra were also examined with the 2nd and 3rd order diffractions of other gratings.

In Fig. 1, the arrangement of the apparatus for a laser-excited single-vibronic-level (SVL) fluorescence is also shown. The flow of the  $\text{He}^* + \text{CF}_2\text{Cl}_2$  reaction products was irradiated downstream from the mixing portion with a pulse laser beam, which was generated by a Molecron UV-14 dye laser system with a Li-formate frequency doubler. The SVL fluorescence

was observed through a Jobin-Yvon H-20 monochromator with a HTV R106UH photomultiplier. By detecting the signal synchronized to the laser pulses, only the emission due to the laser excitation was selectively detected.

## Results and Discussion

**1. General Feature of the Chemiluminescence.** The observed spectrum is shown in Fig. 2. Here vibrational bands are arranged in a long progression with the spacing  $150\text{ cm}^{-1}$ . As will be detailed below, these bands are assignable to the  $\text{A}^1\text{B}_1 \rightarrow \tilde{\text{X}}^1\text{A}_1$  transition of the  $\text{CF}_2$  molecule. Besides these, the 0-0 transition of the  $\text{CF } \tilde{\text{A}}^2\Sigma^+ \rightarrow \tilde{\text{X}}^2\Pi$  system<sup>7)</sup> was observed in the vicinity of 247.6 nm (see also Fig. 3). The  $\Delta v=0$  and  $\Delta v=1$  transitions of the  $\text{C}_2$  Deslandres-d'Azambuja system<sup>8)</sup> were also observed near 385.2 and 360.7 nm, respectively (Fig. 4). The strong atomic line at 388.9 nm (Fig. 4) was attributable to the  $\text{He } ^3\text{P} \rightarrow ^3\text{S}$  transi-

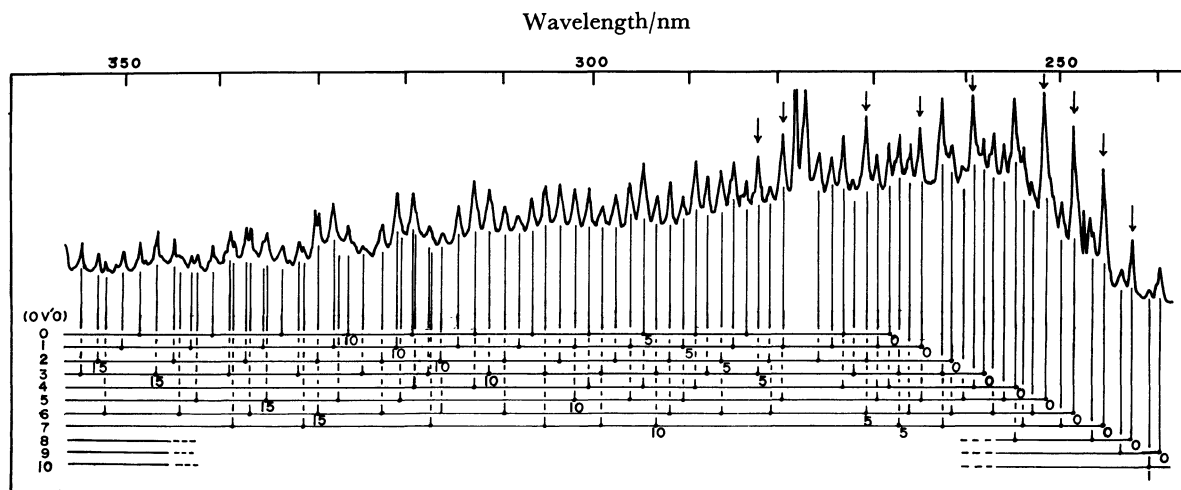


Fig. 2. Chemiluminescence spectrum of the  $\text{CF}_2\text{Cl}_2 + \text{He}^*$  system. Photo-trace of a spectrogram with a dispersion 0.52 nm/mm (the 1st order diffraction from a 300 nm blaze 590 grooves/mm grating), with a slitwidth  $20\text{ }\mu\text{m}$ , and with 8 h exposure. The arrows indicate bands for which K-subband structure were observed.

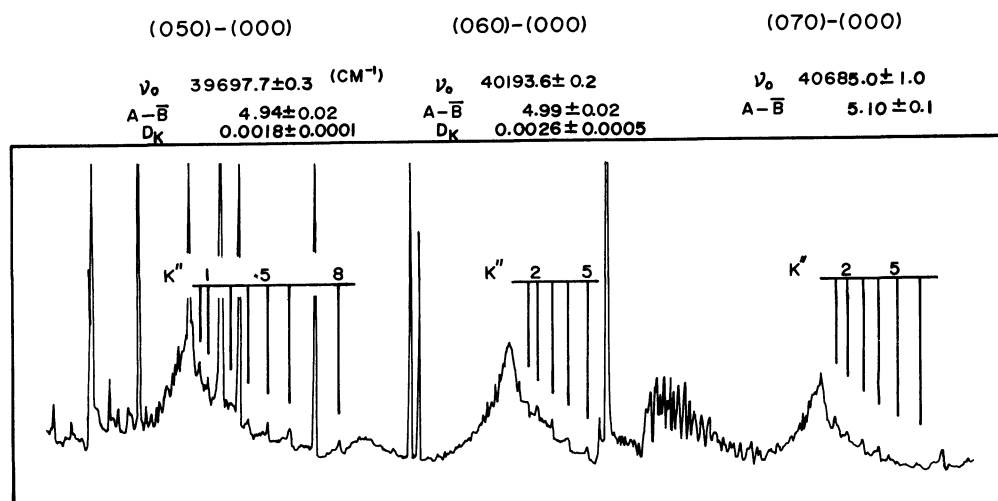


Fig. 3. Chemiluminescence spectrum of the  $\text{CF}_2\text{Cl}_2 + \text{He}^*$  system. Photo-trace of a spectrogram with a dispersion 0.17 nm/mm (the 3rd order diffraction from a 1000 nm blaze 590 grooves/mm grating) and slitwidth  $100\text{ }\mu\text{m}$ .

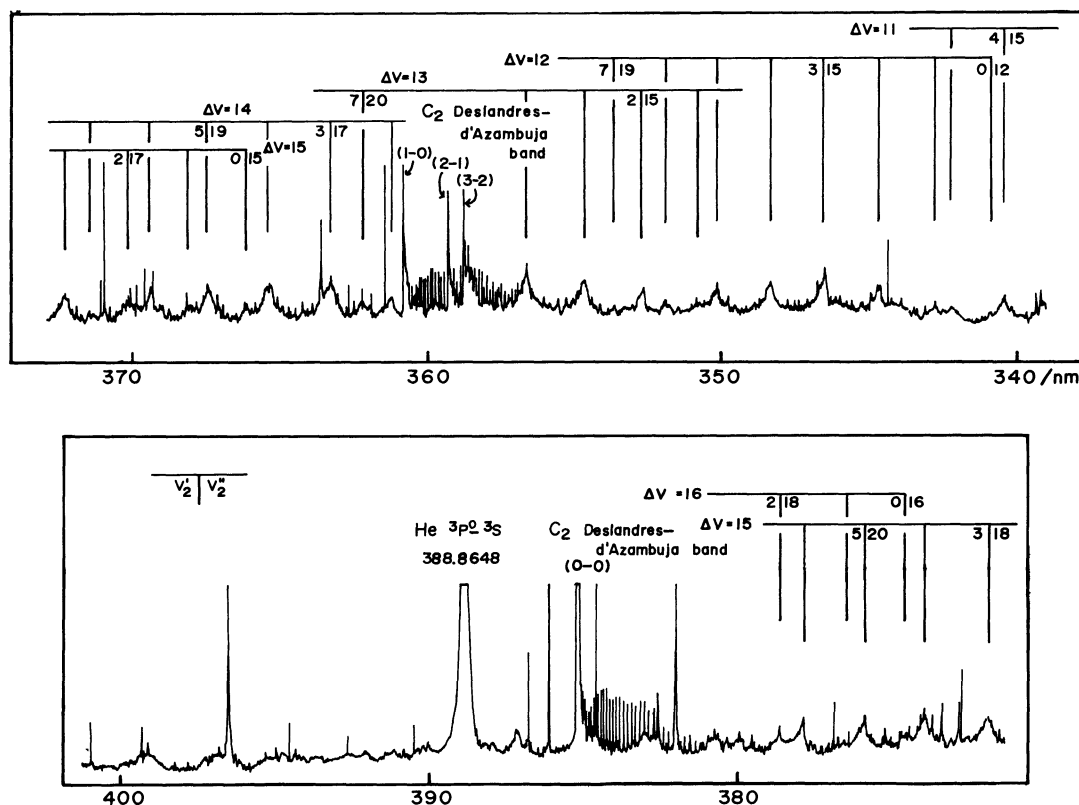


Fig. 4. Chemiluminescence spectrum of the CF<sub>2</sub>Cl<sub>2</sub>+He\* system. Photo-trace of a spectrogram with a dispersion 0.24 nm/mm (the 2nd order diffraction from a 750 nm blaze 590 grooves/mm grating), with a slitwidth 20  $\mu$ m, and with 13 h exposure.

tion.<sup>9)</sup> It is certain that there is the metastable <sup>3</sup>S species involved in the reaction, which has by 19.8 eV higher energy than its ground state, and whose lifetime is a few second at 1 Torr.

## 2. Rotational Structures of the 2<sub>0</sub><sup>5</sup>, 2<sub>0</sub><sup>6</sup>, and 2<sub>0</sub><sup>7</sup> Bands.

On the basis of a comparison with the absorption spectrum  $\tilde{A}^1B_1 \leftarrow \tilde{X}^1A_1$  of CF<sub>2</sub> reported by Mathews,<sup>4)</sup> the vibrational bands in the spectral region 240–270 nm, are all assignable to CF<sub>2</sub>. In a higher dispersion (0.17 nm/mm) spectrogram (Fig. 3), a K-subband structure for  $\Delta K=+1$  was found in each of the 2<sub>0</sub><sup>5</sup>, 2<sub>0</sub><sup>6</sup>, 2<sub>0</sub><sup>7</sup>, and 2<sub>0</sub><sup>8</sup> bands. Here 2 means the  $\nu_2$  (bending) vibration and the super- and subscripts mean the vibrational quantum numbers of the upper and lower electronic states, respectively, in the transition. The peak positions  $\nu_0^{\text{ub}}$  are fitted with the equation for a perpendicular-type transitions,

$$\nu_0^{\text{ub}} = \nu_0 + (A' - \bar{B}') + 2(A' - \bar{B}')K + [(A' - \bar{B}') - (A'' - \bar{B}'')]K^2 - D'_k(K+1)^4 + D''_kK^4, \quad (1)$$

and the band center  $\nu_0$ , the rotational constant  $A' - \bar{B}'$ , and the centrifugal distortion constant  $D'_k$  of the upper state have been determined as given in the upper part of Fig. 3. The  $A'' - \bar{B}''$  value for  $\nu_2''=0$  was fixed at what Mathews determined<sup>4)</sup> (2.5564 cm<sup>-1</sup>). The  $A' - \bar{B}'$  value (4.94  $\pm$  0.04 cm<sup>-1</sup>) thus determined for  $\nu_2'=5$  is in agreement with what was given by Mathews<sup>4)</sup> (4.879  $\pm$  0.003 cm<sup>-1</sup>) within our experimental error. The  $A' - \bar{B}'$  values for  $\nu_2'=6$  and 7 are now newly obtained. It has been found that  $A' - \bar{B}'$  becomes

greater with  $\nu_2'$ .

## 3. Vibrational Structure in the 270–360 nm Region.

The vibrational bands in this spectral region are all explained as progression of the bending mode ( $\nu_2$ ) belonging to the same electronic transition  $\tilde{A}^1B_1 - \tilde{X}^1A_1$ . The assignments are given in Fig. 2. By assuming that observed frequencies ( $\nu$ ) are given as

$$\nu = \nu_{00} + \nu'\nu_2' - \nu'x'\nu_2'^2 - \nu''\nu_2'' + \nu''x''\nu_2''^2, \quad (2)$$

and by the use of the observed 81 transitions, the values of parameters,  $\nu'$  (bending frequency in  $\tilde{A}$ ),  $\nu'x'$  (anharmonicity constant in  $\tilde{A}$ ),  $\nu''$  (bending frequency in  $\tilde{X}$ ), and  $\nu''x''$  (anharmonicity constant in  $\tilde{X}$ ) were determined. The results are given in Table 1, where the deviations of the frequencies calculated on these parameters from the observed ones are also shown. These values explain the total of 135 vibrational transitions with quantum numbers  $\nu_2'=0-10$ ,  $\nu_2''=0-17$  in a whole region we observed.

## 4. Vibrational Structure in the 360–400 nm Region.

The spectrum observed with a higher dispersion in this spectral region is illustrated in Fig. 4. The structure appears at first sight to be of different type from that in the 270–360 nm region. Actually, however, all the bands are explained by taking the  $\nu_2$  vibration in the  $\tilde{A}^1B_1$  state of CF<sub>2</sub> into account; the observed frequencies here also fit with Eq. 2, as those in the 270–360 nm region. The apparent difference is found to be caused by the fact that the spectral region 360–400 nm involves greater  $\Delta\nu$  (=11–16) transitions whereas the 270–360

TABLE 1. VIBRATIONAL BANDS IN THE 270—360 nm REGION OF THE CHEMILUMINESCENCE

Observed frequency $\nu/\text{cm}^{-1}$	$\nu'$	$\nu''$	Obsd— Calcd <sup>a)</sup>	$\nu'$	$\nu''$	Obsd— calcd <sup>a)</sup>	Observed frequency $\nu/\text{cm}^{-1}$	$\nu'$	$\nu''$	Obsd— Calcd <sup>a)</sup>	$\nu'$	$\nu''$	Obsd— Calcd <sup>a)</sup>
41680.4	9	0	18.4				33078.2	1	7	6.4	5	10	—7.8
41500.6	10	1	—0.1				32908.6	2	8	—0.5	6	11	—21.9
41168.1	8	0	6.4				32752.1	3	9	3.6	7	12	—25.0
41002.5	9	1	3.1				32587.6	0	7	7.8	4	10	—2.3
40674.2	7	0	11.7				32422.2	1	8	6.1	5	11	—11.2
40451.2	8	1	—47.9				32250.6	2	9	—3.9	6	12	—28.3
40174.6	6	0	10.3				32103.7	3	10	8.9	7	13	—22.8
39950.5	7	1	—49.4				31911.7	0	8	—12.5	4	11	—25.6
39676.8	5	0	9.6				31816.2	1	9	54.7	5	12	—34.4
39473.3	6	1	—28.4					9	15	—11.5			
39323.1	7	2	—15.2				31591.0	6	13	—37.3			
39177.9	4	0	6.8	8	3	1.0	31566.8	2	10	—34.0			
39011.2	5	1	6.7	9	4	—6.3	31451.6	7	14	—25.2			
38844.1	3	2	4.0				31427.9	3	11	—14.3			
38690.9	3	0	20.9	7	3	13.3	31293.6	4	12	7.9			
38522.0	4	1	13.6	8	4	4.7	31264.8	0	9	—4.8			
38319.7	5	2	—23.2				31147.6	5	13	16.5			
38178.0	2	0	—4.0	6	3	—1.5	31100.8	1	10	—7.1			
38019.4	3	1	6.0	7	4	1.4	30953.5	2	11	5.3	6	14	—25.2
37680.4	1	0	—8.6				30745.3	3	12	—45.3			
37526.9	2	1	7.5	6	4	7.1	30657.0	8	16	—22.8			
37357.7	3	2	5.9	7	5	—1.7	30617.0	0	10	1.1			
37189.2	4	3	3.0	0	0	—7.9	30509.1	5	14	27.6			
37010.4	1	1	—16.0	5	4	—12.3	30460.4	1	11	5.2			
36892.1	2	2	34.3	10	8	1.7	30311.9	2	12	15.3	6	15	—18.1
36528.2	0	1	—6.3	4	4	1.6	30160.6	7	16	—20.0	3	13	20.6
36673.5	3	3	—17.7				30118.3	3	13	—21.7			
36362.4	1	2	—2.4	5	5	—1.7	29960.4	0	11	—3.9	4	14	—25.0
36204.8	2	3	7.7	6	6	1.2	29806.9	5	15	—26.0	1	12	3.3
35696.8	1	3	—7.4	5	6	—9.7	29789.8	1	12	—13.8	10	19	45.2
35539.2	6	7	—7.8				29659.9	6	16	—22.5			
35509.6	2	4	—27.9	6	7	—37.4	29626.8	2	13	—19.2			
35369.6	3	5	—3.3	7	8	—20.0	29514.8	7	17	—19.2			
35205.5	0	3	—6.8	8	9		29471.4	3	14	—19.0			
35040.3	1	4	—4.3				29317.6	0	12	5.9			
34878.9	2	5	0.0	6	8	—12.5	29177.9	5	16	—7.4			
34719.2	3	6	3.9				29131.7	1	13	—21.3			
34547.7	0	4	—4.9	4	7	—6.1	28999.4	6	17	—35.4			
34384.1	1	5	—1.8	5	8	—10.1	28972.8	2	14	—23.5			
34220.0	2	6	—1.3	6	9	—16.8	28823.1	3	15	—18.6			
34062.8	3	7	4.1	7	10	—18.5	28670.7	0	13	9.6			
33886.6	0	5	—7.4	4	8	—11.5	28531.1	1	14	27.7			
33719.9	1	6	—8.4	5	9	—19.7	28389.9	6	18	—0.3			
33558.7	2	7	—6.0	6	10	24.4	28328.1	2	15	—19.6			
33397.4	3	8	—5.7	7	11	—31.3	28175.2	3	16	—18.9			
33243.2	0	6	6.8	4	9	—0.3	28022.7	0	14	11.2	4	17	—19.8

a) Deviations of the frequencies calculated on Eq. 2, with  $\nu_{00}=37197.1(\pm 3.8) \text{ cm}^{-1}$ ,  $\nu'=491.4(\pm 1.4) \text{ cm}^{-1}$ ,  $\nu'x'=-0.52(\pm 0.16) \text{ cm}^{-1}$ ,  $\nu''=663.1(\pm 0.9) \text{ cm}^{-1}$ , and  $\nu''x''=0.50(\pm 0.06) \text{ cm}^{-1}$ .

nm region only smaller  $\Delta\nu(\leq 11)$  transitions. The observed frequencies are given in Table 2, with those calculated on the same set of parameters as what was used for the 270—360 nm region.

5. *SVL Fluorescence of CF<sub>2</sub>*. This experiment was attempted to confirm the assignments so far made to the vibrational bands in the chemiluminescence spectrum. The  $\text{He}^* + \text{CF}_2\text{Cl}_2$  reaction system was

irradiated with a laser beam of 255.10 nm or 251.92 nm. The 255.10 nm beam is now known to correspond to the  $2^4_1$  transition of  $\text{CF}_2$ , and therefore should repopulate the  $v'_2=4$  level of the  $\tilde{A}^1B_1$  state of  $\text{CF}_2$ . Because the radiative lifetime of this level is  $61 \pm 3 \text{ ns}^{10)}$  which is much shorter than the vibrational relaxation time (at 1 Torr), a fluorescence only from this level (SVL fluorescence) should now be observed.

TABLE 2. VIBRATIONAL BANDS IN THE 340—380 nm REGION OF THE CHEMILUMINESCENCE (CF<sub>2</sub>)

Observed frequency, $\nu/\text{cm}^{-1}$	Assignment		Obsd—Calcd <sup>a)</sup> $\text{cm}^{-1}$
	$\nu'$	$\nu''$	
29303.7	4	15	-33.1
29164.6	5	16	-20.7
29120.8	1	13	-32.3
28972.9	2	14	-23.5
28830.1	3	15	-11.6
28687.3	4	16	-1.8
28553.4	5	17	14.8
28499.5	1	14	-3.9
28416.5	6	18	26.3
28296.0	2	15	-51.7
28224.1	7	19	-19.7
28159.2	3	16	-34.9
28008.9	4	17	-33.7
27680.2	2	16	-20.0
27611.7	7	20	11.6
27537.0	3	17	-10.5
27385.4	4	18	-11.5
27334.7	0	15	-28.1
27244.6	5	19	-3.8
27203.7	1	16	-3.4
27089.3	6	20	-12.6
27036.4	2	17	-17.1
26953.5	7	21	-4.0
26891.5	3	18	-10.3
26745.6	4	19	-6.7
26702.6	0	16	-12.6
26609.5	5	20	4.7
26569.6	1	17	9.1
26477.7	6	21	18.4
26421.4	2	18	13.6

a) Deviations of the frequencies calculated on Eq. 2, with the same values of the parameters:  $\nu_{00}$ ,  $\nu'$ ,  $\nu'x'$ ,  $\nu''$ , and  $\nu''x''$ ; as those used for the 270—360 nm region (Table 1).

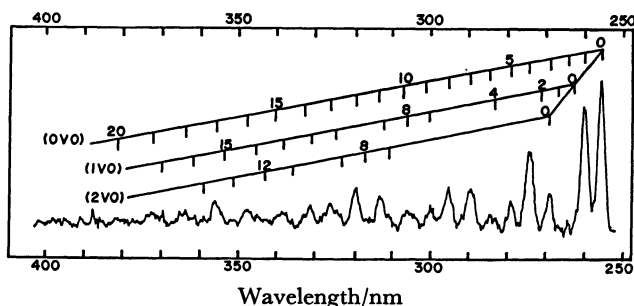


Fig. 5. A single-vibronic-level (SVL) fluorescence spectrum of CF<sub>2</sub>, produced by the CF<sub>2</sub>Cl<sub>2</sub>+He\* reaction. The ground state CF<sub>2</sub> molecule was excited to the  $v_2'=4$  level of the electronic  $\tilde{A}^1B_1$  state by a 255.10 nm laser beam, and the fluorescence spectrum was observed.

This is shown in Fig. 5. As is seen here, a long progression assignable to  $2_2^4$ , (where  $v''=0, 1, 2, \dots, 20$ ) is found to cover the 240—400 nm region. Likewise, a long progression  $2_2^5$ , was found on the 251.92 nm

irradiation, which corresponds to the  $2_2^5$  excitation of this electronic system. These results support the idea that the He\*+CF<sub>2</sub>Cl<sub>2</sub> chemiluminescence is solely caused by the  $\tilde{A}^1B_1$ - $\tilde{X}^1A_1$  transition, not only in the 240—360 nm region but also in the 360—400 nm region.

After we have completed this SVL fluorescence experiment, a similar SVL work on CF<sub>2</sub> independently made by King *et al.*<sup>10)</sup> was published. They prepared CF<sub>2</sub> in a different method from ours, but their SVL fluorescence spectra are in agreement with ours.

6. *Effect of Magnetic Field.* If there is any triplet-state contribution of CF<sub>2</sub> involved in the chemiluminescence spectrum, this would be detected by examining it in a magnetic field. With this expectation in mind, we have observed the chemiluminescence from the He\*+CF<sub>2</sub>Cl<sub>2</sub> system placed in a 5.3 kG magnetic field (see upper-right corner of Fig. 1). In the vibronic and ro-vibronic bands of CF<sub>2</sub>, so far mentioned, however, detectable broadening or intensity shift, as was seen in the case of SO<sub>2</sub> and CS<sub>2</sub>,<sup>22)</sup> was not observed with our optical resolution of about 0.5 cm<sup>-1</sup>. Thus, the assignments of these bands to the singlet-singlet transition ( $\tilde{A}^1B_1$ - $\tilde{X}^1A_1$ ) of CF<sub>2</sub> are again supported here. An appreciable effect has been found, on the other hand, in the relative amounts of the reaction products. In the magnetic field, all of the  $\Delta v=1$  (1-0, 2-1, 3-2, and 4-3) C<sub>2</sub> systems appear as very strong series of lines, while in the spectrum without magnetic field many of these lines are buried in the CF<sub>2</sub> bands. As is shown in Fig. 6, the 247.6 nm band of CF becomes much stronger in the magnet; the intensity ratio of the CF(0-2) over CF<sub>2</sub>(6-0) is doubled by the 5.3 kG field.

7. *Intensity Distribution among the Vibrational Bands.* Having established the assignments of practically all of the vibrational bands in the chemiluminescence

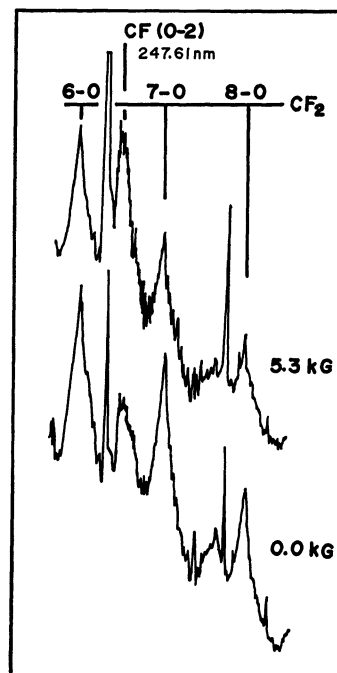


Fig. 6. Chemiluminescence spectrum of the CF<sub>2</sub>Cl<sub>2</sub>+He\* system, with (5.3 kG) and without a magnetic field. Photo-trace of spectrograms with a dispersion 0.52 nm/mm and with a slitwidth 20  $\mu\text{m}$ .

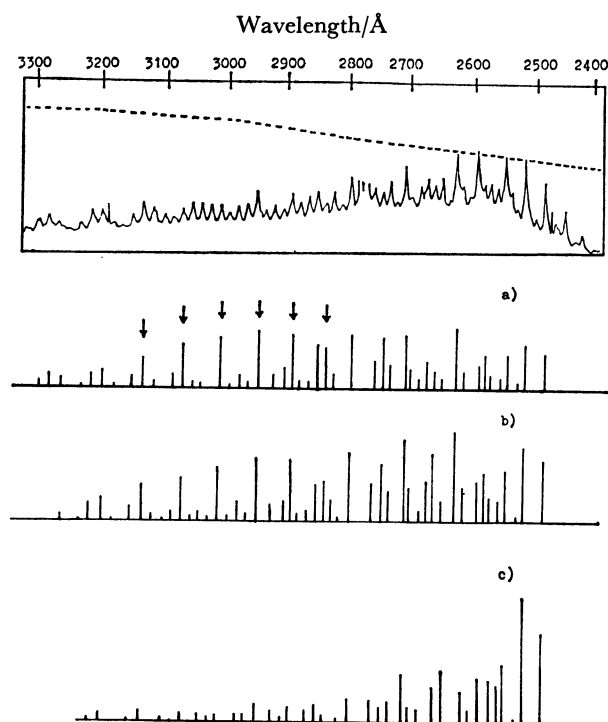


Fig. 7. Observed and calculated intensity distributions among the vibrational bands in the chemiluminescence spectrum of the  $\text{CF}_2\text{Cl}_2 + \text{He}^*$  system. Top: observed with a 3.4 m Jarrel-Ash spectrometer, a 300 nm blaze 590 grooves/mm grating (1st order), 100  $\mu\text{m}$  (entrance) and 150  $\mu\text{m}$  (exit) slitwidths, an HTV R106 UH photomultiplier, and a PAR 5203 lock-in amplifier. The broken line indicates the relative spectral sensitivity of the monochromator and photomultiplier system used in the measurement. Lower three: calculated on the assumptions that the population of the  $\text{CF}_2^*$  molecules in each vibrational level in the excited electronic state  $\tilde{A}^1\text{B}_1$  is given by a) the Boltzmann distribution at 2100 K, b) the Boltzmann distribution at 3000 K, and c) the distribution shown by the white circles in Fig. 8, which was reached by the least squares fit (that is detailed in the text). The arrows indicate the vibrational bands  $2v''$  ( $v''=3, 4, 5, 6, 7$ , and  $8$ ), whose intensities are too great on the assumption a) or b).

spectrum, we now proceed to an examination of their intensities. The relative intensities were determined by the use of photoelectronic detection system described above, and the results are shown in Fig. 7 (top). Theoretically, on the other hand, the intensity  $I(v'_2, v''_2)$  of the band corresponding to the  $\tilde{A}^1\text{B}_1, v'_2 \rightarrow \tilde{X}^1\text{A}_1, v''_2$  transition is given as

$$I(v'_2, v''_2) \propto S(\nu) N(v'_2) \nu^4 |\langle v'_2 | v''_2 \rangle|^2, \quad (3)$$

where  $S(\nu)$  is the spectral response of the monochromator and detector system,  $N(v'_2)$  is the population in the vibrational ( $0v'_20$ ) level of the electronic  $\tilde{A}^1\text{B}_1$  state of  $\text{CF}_2$ ,  $\nu$  is the transition frequency, and  $\langle v'_2 | v''_2 \rangle$  is the Franck-Condon overlap integral.

For  $S(\nu)$ , the efficiency-wavelength curve of the grating and spectral response of the photomultiplier (given by the manufacturer) were taken into account. The ultimate  $S(\nu)$  value assumed here is given in Fig. 7,

(top) with broken line. The  $\langle v'_2 | v''_2 \rangle$  values were obtained primarily from the SVL fluorescence experiments of ourselves (Section 6) as well as of King *et al.*<sup>10)</sup> Where the experimental values are not available ( $v' \geq 7$ ), however, the Franck-Condon overlap integrals were estimated by a calculation on the basis of the geometry and vibrational frequencies of the  $\text{CF}_2$  molecule both in  $\tilde{A}^1\text{B}_1$  and  $\tilde{X}^1\text{A}_1$  states.<sup>4)</sup> In the calculation, the effect of anharmonicity (detectable in the observed frequencies) was first taken into account. The effect, however, has been found to be very small on the Franck-Condon integrals; each perturbed eigenfunction was found to be practically equal to the corresponding unperturbed eigenfunction, the amount of contribution from other unperturbed eigenfunctions being less than 0.1%. Therefore, the effect has finally been ignored. The calculation was made in the two-dimensional space involving the symmetric stretching as well as the bending modes, in order to take a probable Duschinsky effect into account.<sup>11,12)</sup> The calculation was made by the method of Sharp and Rosenstock.<sup>13)</sup> A computer program prepared by Professor A. J. Merer (University of British Columbia) was used after some modifications. To reach a proper set of vibrational modes we need a proper set of force constants. In the ground state  $\tilde{X}$ , this can be fixed by the use of the centrifugal distortion constants obtained by a microwave spectral study.<sup>14)</sup> For the excited state  $\tilde{A}$ , the values of inertial defects<sup>4)</sup> in the (000) and (010) states,  $\Delta(000)=0.138 \text{ amu} \cdot \text{\AA}^2$ , and  $\Delta(010)=0.314 \text{ amu} \cdot \text{\AA}^2$ , were used to fix the force constants, in combination with Oka-Morino equation<sup>15)</sup> and Meal-Polo equation.<sup>16)</sup>

Only the  $N(v'_2)$  values are now left unknown in Eq. 3. As a first trial, a Boltzmann distribution was assumed for  $N(v'_2)$ . As may be seen in Figs. 7(a) and (b), however, this causes a serious disagreement between the observed intensity distribution and what is calculated on Eq. 3. The observed chemiluminescence spectrum indicates that relative value of  $N(v'_2=0)$  is greatly lower than what is expected from a Boltzmann distribution.

#### 8. Population Distribution $N(v'_2)$ among Vibrational Levels of a Nascent $\text{CF}_2^*$ .

The relative values of  $N(v'_2)$  were next determined so as to reach the best fit between the observed intensity distribution among the vibrational bands (Fig. 7, top) and what is calculated on Eq. 3. What are obtained by a least squares method are shown in Fig. 8 with white circles. In this procedure, the values of  $N(5)$ ,  $N(6)$ ,  $N(7)$ ,  $N(8)$  are well fixed, because  $2v''$  bands with  $v'_2=5, 6, 7$ , and  $8$  are all well isolated from other bands. While, the uncertainties for the values of  $N(0)$ ,  $N(1)$ ,  $N(2)$ , and  $N(4)$  are great (see the error bars in Fig. 8), because every  $2v''$  band overlaps with  $2v''+3$  band in the 280–323 nm region. Especially, the fixing of the  $N(3)$  value was not found to be practical, because every  $2v''$  band overlaps with  $2v''+3$  band; here no experimental values are available of the Franck-Condon overlap integrals  $\langle 7 | v''+3 \rangle$ , and very reliable calculations for the Franck-Condon overlap integrals with higher  $v'$  and  $v''$  are not practical.

In spite of such an ambiguity, however, it is now quite certain that the initial-state ( $\tilde{A}^1\text{B}_1$ ) population  $N(v')$  in the chemiluminescence, now in question, is

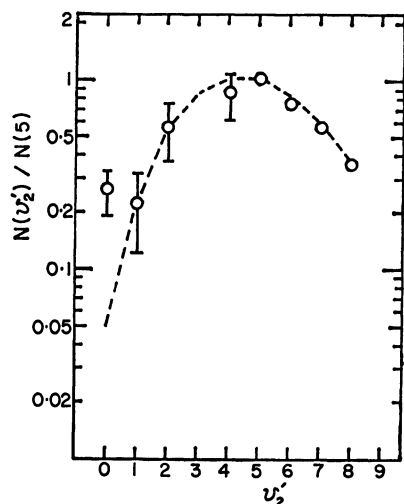


Fig. 8. The population of the CF<sub>2</sub>\* molecules, produced by the CF<sub>2</sub>Cl<sub>2</sub>+He\* reaction, in each vibrational level ( $v'_2=0, 1, \dots$ , or 8) in the excited electronic state  $\tilde{A}^1B_1$ . White circle: determined by a least squares fit with the observed intensities of the vibrational bands in the 240–330 nm region of the CF<sub>2</sub>Cl<sub>2</sub>+He\* chemiluminescence spectrum. Broken line: calculated on an assumption that the change from the CF<sub>2</sub> moiety of CF<sub>2</sub>Cl<sub>2</sub> into CF<sub>2</sub>\* (caused by a collision with He\* and by throwing Cl<sub>2</sub> away) takes place according to the Franck-Condon principle, i.e., vertically upward in the potential energy diagram with the FCF angle along the abscissa.

distributed among the vibrational levels with a great deviation from a Boltzmann distribution. Instead, it shows a maximum at  $v'_2=5$ . Since the radiative lifetime of the vibronic levels of the  $\tilde{A}^1B_1$  state of CF<sub>2</sub> is  $61 \pm 3$  ns,<sup>10</sup> and since this is much shorter than the vibrational relaxation time ( $\approx 5 \mu s$ ) at 1 Torr, the population distribution  $N(v')$  just found is considered to be exactly what is produced by the CF<sub>2</sub>Cl<sub>2</sub>+He\* reaction.

9. On the CF<sub>2</sub>Cl<sub>2</sub>+He\* Reaction Mechanism. The observed  $N(v')$  versus  $v'$  relation (Fig. 7) is concerned with the mechanism of the CF<sub>2</sub>\* production. The result suggests that the scission of the CF<sub>2</sub>Cl<sub>2</sub> molecule into CF<sub>2</sub>\*+Cl<sub>2</sub>\* (caused by a collision with the metastable He\*) takes place so rapidly that no vibration of the CF<sub>2</sub> moiety occurs during this process. The FCF angle of the ground-state CF<sub>2</sub>Cl<sub>2</sub> molecule is  $105.4 \pm 1.0^\circ$  determined by microwave study<sup>21</sup> and this would tend to be retained in the product when the reaction is sufficiently rapid. This means that the product tends to have a greater population in a higher level of the bending vibration, because the equilibrium FCF angle of the product CF<sub>2</sub>\* ( $122^\circ$ ) is greatly different from  $105.4^\circ$ . Let us tentatively assume that the CF<sub>2</sub>Cl<sub>2</sub>→CF<sub>2</sub>\*+Cl<sub>2</sub>\* change takes place according to the Franck-Condon principle.<sup>17</sup> By assuming that the CF<sub>2</sub> bending is a harmonic oscillation both in the reactant (ground state CF<sub>2</sub>Cl<sub>2</sub> molecule) and the product (excited  $\tilde{A}^1B_1$  CF<sub>2</sub> radical), and that their frequencies are  $458^{18}$  and  $491 \text{ cm}^{-1}$  (our value), respectively, one-dimensional Franck-Condon overlap (reactant-product) integrals were calculated. The squares of these integrals are to be

compared with the observed populations  $N(v')$ . What were calculated (given in Fig. 8 by broken line) agree with the observed populations, if  $\Delta Q_2$  is assumed to be  $0.88 \text{ \AA amu}^{1/2}$ . Here  $\Delta Q_2$  is the shift of the potential minimum in the bending normal coordinate  $Q_2$  in the reactant (CF<sub>2</sub>Cl<sub>2</sub>) from that in the product (CF<sub>2</sub>\*). This  $\Delta Q_2$  value corresponds to a shift of about  $18^\circ$  in the FCF angle (i.e.,  $\angle FCF = 122 - 18 = 104^\circ$ ); this is fairly close to what is expected in the simple model (the CF<sub>2</sub>\* and CF<sub>2</sub>Cl<sub>2</sub> difference in  $\angle FCF$  is  $122.3^\circ - 105.4^\circ = 16.9^\circ$ ).

Lastly, let us take a look at the energy balance in the reaction. On the basis of a thermochemical data,<sup>19</sup> approximately 8.8 eV is considered to be required to dissociate the CF<sub>2</sub>Cl<sub>2</sub> molecule into CF<sub>2</sub> and Cl<sub>2</sub> and then to excite CF<sub>2</sub> up to CF<sub>2</sub>\* ( $\tilde{A}^1B_1$ ). Because He\* ( $^3S_0$ ) has 19.8 eV, an excess energy of 2.6 eV is available, even if the Cl<sub>2</sub> molecule takes 8.4 eV to excite itself to  $\tilde{D}^3\Pi_{1g}$ .<sup>20</sup> The excess energy would be converted into the translational energy of the products (CF<sub>2</sub>\*+Cl<sub>2</sub>\*+He), so that Cl<sub>2</sub>\* would be rapidly removed from the CF<sub>2</sub>\* moiety after the reaction.

We wish to express our sincere thanks to Professor Saburo Nagakura, the University of Tokyo, for his kindness extended in our use of Jarrel-Ash spectrograph as well as for his valuable discussions. Our thanks are also due to Professor A. J. Merer, the University of British Columbia, for the computer program used in our calculation of two-dimensional Franck-Condon overlap integrals. This work was supported partly by a Grant-in-Aid for Scientific Research No. 354153 from the Ministry of Education, Science and Culture.

## References

- 1) The present article is a part of T. Ishiguro's Doctor Thesis, The University of Tokyo, Japan, 1980.
- 2) D. S. Y. Hsu, M. E. Umstead, and M. C. Lin, Fluorine Containing Free Radicals, Kinetics, and Dynamics of Reactions, A. C. S. Symposium Series (No. 66), American Chem. Soc., Washington (1978).
- 3) P. Venkateswarlu, *Phys. Rev.*, **77**, 676 (1950).
- 4) C. W. Mathews, *Can. J. Phys.*, **45**, 2355 (1967).
- 5) Quach-Tat-Trung, G. Durocher, P. Sauvageau, and C. Sandorfy, *Chem. Phys. Lett.*, **47**, 404 (1977).
- 6) S. Koda, *Chem. Phys. Lett.*, **55**, 353 (1978).
- 7) T. L. Porter, D. E. Mann, and N. Acquista, *J. Mol. Spectrosc.*, **16**, 228 (1965).
- 8) H. Kopfermann and H. Schweitzer, *Z. Phys.*, **61**, 87 (1930).
- 9) A. R. Striganov, N. S. Sventitskii, Tables of Spectral Lines of Neutral and Ionized Atoms, IFI/Plenum, New York (1968).
- 10) D. S. King, P. K. Schenck, and J. C. Stephenson, *J. Mol. Spectrosc.*, **78**, 1 (1979).
- 11) F. Duschinsky, *Acta Physicochim. URSS*, **1**, 551 (1937).
- 12) G. J. Small, *J. Chem. Phys.*, **54**, 3300 (1971).
- 13) T. E. Sharp and H. M. Rosenstock, *J. Chem. Phys.*, **41**, 3453 (1964).
- 14) W. H. Kirchhoff, D. R. Lide, Jr., and F. X. Powell, *J. Mol. Spectrosc.*, **47**, 491 (1973).
- 15) T. Oka and Y. Morino, *J. Mol. Spectrosc.*, **8**, 9 (1962).
- 16) J. H. Meal and S. R. Polo, *J. Chem. Phys.*, **24**, 1126 (1956).

- 17) J. F. Prince, C. B. Collins, and W. W. Robertson, *J. Chem. Phys.*, **40**, 2619 (1964).
  - 18) T. Shimanouchi, Tables of Molecular Frequencies, Consolidated Vol. II, *J. Phys. Chem.*, Reference Data, **6**, (3) (1977).
  - 19) E. N. Okafo and E. Whittle, *J. Chem. Soc., Faraday Trans. 1*, **70**, 1366 (1974).
  - 20) G. Herzberg, "Spectra of Diatomic Molecules," Van Nostrand Company, Princeton, N. J. (1950), p. 519.
  - 21) C. F. Su and E. L. Beeson, Jr., *J. Chem. Phys.*, **66**, 330 (1977).
  - 22) A. E. Douglas, *Can. J. Phys.*, **36**, 147 (1958).
-